

# Investigation of structural states and oxidation processes in $\text{Li}_{0.5}\text{Fe}_{2.5}\text{O}_{4-\delta}$ using TG analysis

A. P. Surzhikov · T. S. Frangulyan ·  
S. A. Ghyngazov · E. N. Lysenko

Received: 14 April 2011 / Accepted: 7 June 2011 / Published online: 25 June 2011  
© Akadémiai Kiadó, Budapest, Hungary 2011

**Abstract** Using the methods of X-ray phase and DSC analyses, a correlation is established between ordering/disordering of the structure of lithium pentaferrite (LPF— $\text{Li}_{0.5}\text{Fe}_{2.5}\text{O}_{4-\delta}$ ) and its nonstoichiometry with respect to oxygen. Ferrite specimens with a reduced content of oxygen were prepared by thermal annealing in vacuum ( $P = 2 \times 10^{-4}$  mmHg). It is shown that this treatment results in oxygen nonstoichiometry and causes a transition of LPF into a state with random distribution of cations in the crystal lattice. Using nonisothermal thermogravimetry (TG), the kinetic dependences of oxygen absorption by the anion-deficient LPF are investigated within the temperature interval  $T = (350\text{--}640)$  °C in the course of its oxidation annealing in air. The kinetic experiment data are processed with the Netzsch Thermokinetics software. The oxidation rate constants, the effective coefficients, and the activation energy of oxygen diffusion in the material under study are derived. Their values are in a satisfactory agreement with those earlier obtained for the lithium–titanium ferrite ceramic material of the following composition:  $\text{Li}_{0.649}\text{Fe}_{1.598}\text{Ti}_{0.5}\text{Zn}_{0.2}\text{Mn}_{0.051}\text{O}_{4-\delta}$ . The effective activation energy of oxygen diffusion in LPF calculated within the temperature interval  $T = (350\text{--}640)$  °C is found to be  $E_d = 1.88$  eV. In its value, it is close to the activation energy of oxygen diffusion along grain-boundaries in the lithium–titanium ferrite ceramic material.

**Keywords** Lithium pentaferrite · Oxygen nonstoichiometry · Diffusion · Activation energy

## Introduction

Lithium pentaferrite (LPF) ( $\text{LiFe}_5\text{O}_8$  or  $\text{Li}_{0.5}\text{Fe}_{2.5}\text{O}_4$ ) is the simplest basic material for a variety of chemical compositions of lithium ferrosinels. LPF has the structure of inverted spinel. Its crystal structure can exist in two forms: ordered (space group  $P4_332$ ) and disordered (space group  $Fd3m$ ) [1–3]. Recently LPF has been in the focus of investigation with an outlook of its practical application in electronic devices for microwave engineering [3, 4], as cathode material for chemical current sources [5], chemical sensors [6], and solid-state electrolytes [7].

It is well known that for a given cation composition the properties of a ferrite ceramic material may vary in a wide range as a function of a number of technological factors (temperature, composition, and gas medium pressure) [3, 4, 8–11]. This variation is due to a significant influence of structure imperfection of the oxygen sublattice of oxide materials on their functional properties.

Generally, ferrosinels do not exhibit ideal stoichiometry. Due to the effective course of redox reactions at elevated temperatures ceramic structures can be formed, which are characterized by either excessive or deficient oxygen content. This inevitably gives rise to a change in the charge state of transition metal ions and, hence, the functional properties of ferrites. This special behavior of ferrosinels is very promising as concerns a deliberate control over their electromagnetic properties.

Since oxygen exchange between the ferrite ceramic materials and the environment has a diffusion nature, the study of diffusion in these materials becomes increasingly important both from the fundamental and applied points of view. There are few works dealing particularly with oxygen diffusion in lithium ferrosinels [12, 13]. Previously [13], we investigated the oxidation kinetics of oxygen-deficient

A. P. Surzhikov · T. S. Frangulyan · S. A. Ghyngazov (✉) ·  
E. N. Lysenko  
Tomsk Polytechnic University, pr. Lenina, 30, 634050 Tomsk,  
Russia  
e-mail: ghyngazov@tpu.ru

lithium–titanium ferrite ceramic materials using thermogravimetry (TG). The oxidation rate constants and the effective coefficients of oxygen diffusion into the ferrites under study were determined. The values of diffusion activation energy derived in that work were consistent with the experimentally obtained [12] activation energy of oxygen diffusion along the grain boundaries in the lithium–titanium ceramic material.

This work continues the previous investigation. The purpose of the present study is to experimentally determine the basic kinetic parameters characterizing the efficiency of oxidation reactions in LPF. To obtain these data is especially challenging to get an insight into the character of the influence that a chemical composition of the cation lattice of lithium ferros spinels exerts on the processes of their oxygen exchange with a gas medium.

### Experimental procedure

Lithium ferrite was synthesized using a standard ceramic-manufacturing process from a mixture of initial components ( $\text{Li}_2\text{CO}_3$  and  $\text{Fe}_2\text{O}_3$ ) of a stoichiometric composition. The procedure for obtaining synthesized ferrite powders (SFP) is detailed in [14].

Bismuth trioxide (2 wt%) was added to the powders thus synthesized. Pellets measuring 18 mm in diameter and 3 mm in thickness were prepared from the resulting mixture, followed by roast-sintering in air at  $T = 1320$  °C for 2 h in a resistance furnace. The heating and cooling rate was 10 °C/min. This roast-sintering mode yielded the ceramic material with higher porosity ( $\theta \approx 11\%$ ). According to the layer-by-layer measurement of electric conductivity of the ceramic samples, their higher porosity favored a more effective and uniform oxidation of the samples, which occurred during cooling, and yielded the ferrite material with the highest oxygen saturation.

The sintered ceramic pellets were ground in an agate mortar. The freshly prepared powders were then screened through a series of sieves to separate a fraction with the grain size up to 40  $\mu\text{m}$ . The volume of the resulting fraction was divided into two halves. The first half was left as-sieved, it was the initial powder termed here as LPF1. The other part was annealed in vacuum (residual gas pressure  $P = 2 \times 10^{-4}$  mmHg) at  $T = 800$  °C for 2 h to produce ferrite material with a reduced content of oxygen. This powder is referred to as LPF2.

The X-ray structure analysis of the powders in question was performed in an ARL X'tra diffractometer using monochromatized  $\text{Cu K}_\alpha$  radiation.

Changes in mass of the samples under study due to their interaction with the gas medium were registered directly in the course of thermal treatment using an STA 449 C

Jupiter Analyzer (Netzsch-Geratebau GmbH, Germany) with the sensitivity of balance 0.1  $\mu\text{g}$ . Use was made of an  $\text{Al}_2\text{O}_3$  crucible shaped as a cup. To ensure accurate baseline measurements, the crucible was loaded with inert powdered  $\text{Al}_2\text{O}_3$ , whose mass was equal to that of the powder under study. Heating was performed in a linear mode at the rates 0.5, 1.0, 5.0, and 8.0 °C/min. For the DSC measurement, the powder sample was heated at a rate of 50 °C/min.

### Experimental results

The first stage of investigation consisted in the X-ray phase and thermal analyses of the initial state of as-prepared samples. For the sake of illustration, shown in Fig. 1a and b are typical X-ray diffraction patterns from the LPF1 and LPF2 powder samples.

A full-profile analysis of the X-ray patterns using a Powder Cell 2.4 software demonstrated that the set of reflections observed in them corresponds to the superposition of reflections from a single spinel phase. The presence of high-intensity superstructure reflections in the diffraction patterns from LPF1 is indicative of ordering of the lithium spinel structure. These reflexes are indicated by asterisks in Fig. 1a. This type of ordering was also characteristic for SFP.

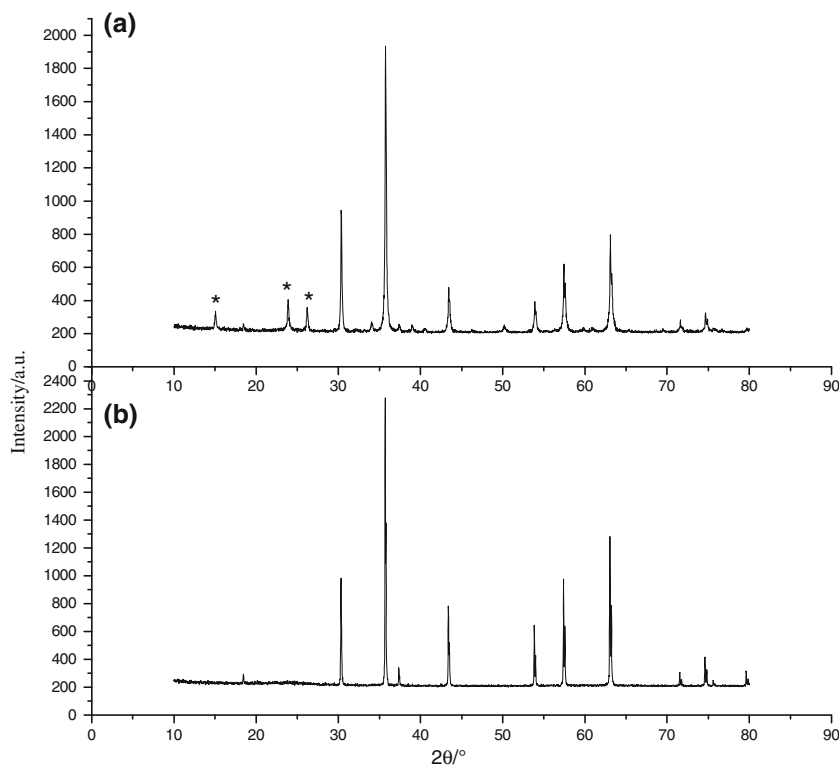
No superstructure reflections were observed in the diffraction pattern from LPF2 (Fig. 1b). This implies that thermal annealing of the powder in vacuum resulted in a distortion of ion ordering and a transition of LPF into a state with random cation distribution in the crystal lattice.

Table 1 lists the lattice parameter values (a) of the materials under study. The values obtained in this work (a) for SFP and LPF1 are in a satisfactory agreement with that typical for lithium ferrite with stoichiometric composition [15, 16]. Note that LPF2 is characterized by a higher lattice parameter value, which indicates a deficit of oxygen in this material [13, 15].

In order to determine the level of oxygen nonstoichiometry in different ferrite powder samples, we analyzed variation of their mass during thermal annealing in air using TG. The annealing runs were performed as follows. The analyzed sample was heated to  $T = 640$  °C at a rate of 3.0 °C/min. This was followed by a long isothermal tempering at this temperature till equilibrium with the gas medium, which was determined from the conservation of the sample mass in the isothermal stage. According to the TG analysis, the interaction of lithium ferrite at this temperature is mostly oxidative in character.

The experiments showed that the mass of the SFP and LPF1 powder samples virtually did not change, while that of the LPF2 powders increased due to absorption of

**Fig. 1** Diffraction patterns from lithium pentaferrite. Initial LPF1 (a) and LPF2 annealed in vacuum at  $T = 800\text{ }^{\circ}\text{C}$  for 2 h (b)



**Table 1** Characteristics of lithium pentaferrite with different levels of oxygen nonstoichiometry

Powder sample	$\Delta m \cdot m^{-1}/\%$	$\Delta \delta/\%$	$a/\text{\AA}$	$T_K/^{\circ}\text{C}$	$T_{\alpha \rightarrow \beta}/^{\circ}\text{C}$	$Q_{\alpha \rightarrow \beta}/\text{J g}^{-1}$	$Q_{\beta \rightarrow \alpha}/\text{J g}^{-1}$
SFP	0	0	8.331	628	752	11.4	12.8
LPF1	0	0	8.3307	627	747	12.8	11.8
LPF2	0.251	0.032	8.334	612	–	0.05	11.5

oxygen. Table 1 lists the values of the relative mass increment and the respective variations of the nonstoichiometry parameter  $\Delta\delta$ , calculated using the formula  $\Delta\delta = (\Delta m/m) \cdot (M/M_o)$ , where  $\Delta m$  is the mass variation during transition from the initial conditions to the state of equilibrium with the gas medium,  $m$  is the oxide mass under the initial conditions,  $M$  is the molecular mass of the oxide under study, and  $M_o$  is the atomic mass of oxygen.

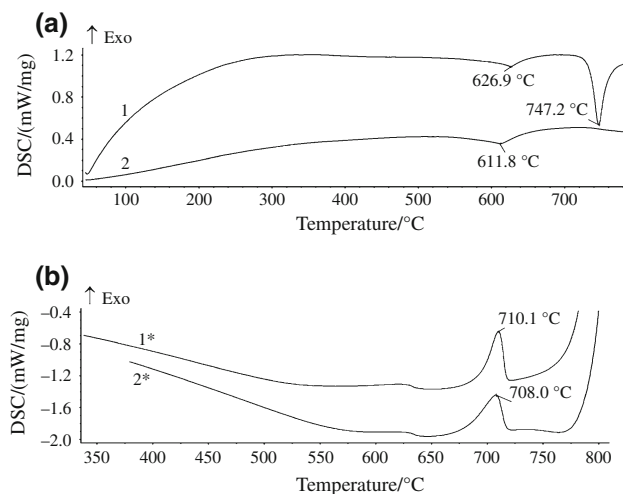
It is evident from the data listed in Table 1 that the LPF2 powder samples are characterized by nonstoichiometry with a deficit of oxygen. It is for this reason that heating gives rise to oxidation of the sample analyzed and results in an increase of its mass. On the other hand, the mass of the samples during annealing is maintained constant. This suggests that SFP and LPF1 have a stoichiometric composition with respect to oxygen.

Figure 2a and b presents typical results of a DSC investigation of lithium ferrites LPF1 and LPF2 under the conditions of heating (Fig. 2a) and cooling (Fig. 2b). The dependences in Fig. 2a and b plotted as curves 1, 1\*, and 2 were obtained during heating and cooling of the powder

samples in a nitrogen flow. It is evident that in the DSC curve from the ferrite of a stoichiometric composition (LPF1) there are two pronounced endothermic peaks (Fig. 2a, curve 1). Similar data were obtained for SFP.

The weak peak at  $T_C = 627\text{ }^{\circ}\text{C}$  corresponds to a magnetic phase transition (ferrimagnetic  $\rightarrow$  paramagnetic). Its position serves a characteristic of the Curie temperature. This is confirmed by the fact that during the TG/DSC measurements in the magnetic field at this temperature there is a stepwise increase in the sample mass due to the destruction of ferromagnetic ordering under the action of heat [14].

A more pronounced high-temperature peak at  $T = 747\text{ }^{\circ}\text{C}$  is associated with a phase transition of the ordered structure of  $\text{Li}_{0.5}\text{Fe}_{2.5}\text{O}_4$  into a disordered state ( $\alpha \rightarrow \beta$  phase transition). The value of enthalpy of the  $\alpha \rightarrow \beta$  transition characterizes the degree of ordering of the structure of lithium spinel. This transition is reversible. Upon cooling, a reverse  $\beta \rightarrow \alpha$  transition is observed and the exothermic peak appearing in curve 1\* (Fig. 2b) corresponds to this transition.



**Fig. 2** DSC dependences obtained during heating (a) followed by cooling (b) of the LPF1 (curves 1 and 1\*) and LPF2 (curves 2 and 2\*) powder samples. Curves 1, 1\*, and 2 were obtained in a nitrogen flow, curve 2\*—in an air flow

When LPF2 samples were investigated using the DSC method, heating was performed in nitrogen, and subsequent cooling in both nitrogen and air. From the data depicted in Fig. 2a (curve 2) it is evident that variation in the oxygen stoichiometry of lithium ferrite shifts the temperature of its magnetic phase transition. Note that there is practically no structural endothermic peak (Fig. 2a, curve 2). It should be underlined that there was no exothermic peak due to the  $\beta \rightarrow \alpha$  transition either, if the gas medium was not changed in the cooling stage. On the other hand, if an LPF2 sample was cooled in air, a strong exothermic peak appeared in the DSC curve (Fig. 2b, curve 2\*), which suggested a transition of the disordered nonstoichiometric lithium ferrite into an ordered state ( $\beta \rightarrow \alpha$  phase transition). These experimental data unambiguously relate the processes of ordering and disordering of the LPF structure to its oxygen stoichiometry.

The values of  $T_C$  and  $T_{\alpha \rightarrow \beta}$ , as well as those of the enthalpy of structural phase transitions ( $Q_{\alpha \rightarrow \beta}$ ) and  $Q_{\beta \rightarrow \alpha}$  for the ferrite powders differing in the content of oxygen are listed in Table 1. These values for the SFP and LPF1 samples are in a satisfactory agreement with the literature data obtained for stoichiometric  $\alpha$ - $\text{Li}_{0.5}\text{Fe}_{2.5}\text{O}_4$  [16–18]. Our results point to a reduced Curie temperature and a lower enthalpy of the  $\alpha \rightarrow \beta$  phase transition in nonstoichiometric lithium ferrite.

In order to produce lithium ferrite in a disordered state at room temperature, use is typically made of fast quenching of the specimens from the sintering temperature ( $T \approx 1000$  °C) [3, 15, 19]. Our experiments demonstrated that the same could be achieved by varying the oxygen nonstoichiometry of lithium ferrite. Below we provide an interpretation of this phenomenon.

Annealing of ferrite at  $T > T_{\alpha \rightarrow \beta}$  destroys the ordered distribution of cations in the octahedral positions. If this treatment is performed at a reduced oxygen pressure, the concentration of oxygen vacancies is concurrently increased due to volatilization of oxygen. Upon cooling of ferrite, a reverse process of ordering proceeds through the stage of formation of the ordered phase nuclei. There is some literature data that an increase in nonstoichiometry with respect to oxygen can significantly prevent nucleation of the ordered phase [3]. Therefore, even if cooling of nonstoichiometric lithium ferrite samples is rather slow, their disordered state could still be maintained given a reduced partial pressure. This standpoint is quite consistent with the fact that for LPF2 the exothermic heat effect  $Q_{\beta \rightarrow \alpha}$  during the  $\beta \rightarrow \alpha$  transition was found to exceed the value of  $Q_{\alpha \rightarrow \beta}$ . This result could be accounted for by the fact that under heating in a nitrogen flow and subsequent cooling in air, nonstoichiometric ferrites absorb oxygen, which restores their oxygen stoichiometry. It is for this reason that upon cooling the material readily transits into an ordered state. The degree of ordering is thus increased, which is indicated by higher values of  $Q_{\beta \rightarrow \alpha}$  compared to  $Q_{\alpha \rightarrow \beta}$ . The series of experiments performed so far provide an idea of the initial state of the nonstoichiometric LPF material under study.

The next stage of the study consisted in determination of kinetic parameters and diffusion characteristics of oxygen absorption in  $\text{Li}_{0.5}\text{Fe}_{2.5}\text{O}_{4-\delta}$  (LPF2). The oxidation annealing runs were performed within the temperature interval (400–640) °C.

Using the method of nonisothermal TG we measured the kinetic changes in the powder sample mass during its heating at different rates.

Note that similarly to the procedure reported in [13] we used a combined heating regime that included nonisothermal and isothermal stages. The sample in question was heated at a certain rate from the temperature  $T = 400$  °C to  $T = 640$  °C. It was then isothermally tempered for a long time at the latter temperature till equilibrium with the gas medium, which was determined from the persistent conservation of the material mass. The kinetic dependences of

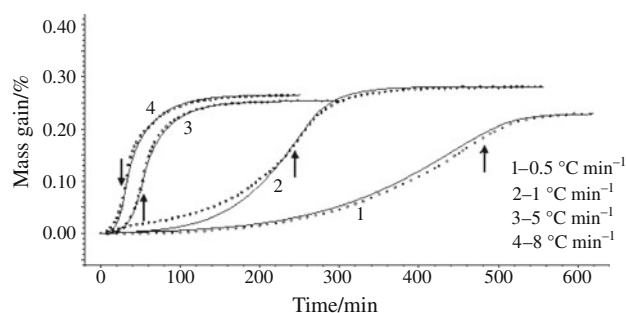


**Fig. 3** Oxidation kinetics of lithium pentaferrite (LPF). Experimental (dots) and calculated (solid lines) data

**Table 2** Calculated values of kinetic and diffusion characteristics of oxidation of lithium ferrites from TG analysis

Material	Kinetic model	Parameter $\log A/s^{-1}$	Parameter $E/kJ\ mol^{-1}$	Parameter $E/eV$	Parameter $D_0/cm^2\ s^{-1}$	Parameter $E_D/eV$
LPF2	$D_{3F}$	5.56	$173.0 \pm 3.93$	$1.79 \pm 0.04$	4.1	1.88
Li–Ti ferrite	$D_{3F}$	4.79	$166.0 \pm 2.26$	$1.72 \pm 0.02$	2.25	1.89

mass variation of the ferrite powder sample during heating at different rates are plotted in Fig. 3. The arrows show the time points of a transition from the nonisothermal heating mode to the nonisothermal tempering.

The results of this kinetic experiment were processed using a licensed Netzsch Thermokinetics software developed specially for the users of devices manufactured by the Netzsch-Geratebau GmbH. The key points of the software program are reported in [20].

An analysis showed that the  $D_{3F}$  model (Fick's 3D diffusion model) provides the most satisfactory description of the resulting kinetic dependences. The calculated kinetic parameters are listed in Table 2, and the curves constructed with these parameters are plotted in Fig. 3.

The algorithm for calculating the diffusion characteristics was described earlier [13]. It consisted of the construction of kinetic dependences of the degree of transformation  $\alpha = f(t)$  for isothermal conditions from the known reaction-rate constants. This was done using the Netzsch Thermokinetics software. Parameter  $\alpha$  represented a ratio of the current mass increase to the maximum possible mass increase, which corresponded to oxidation of the lithium spinel up to a stoichiometric state.

The reaction of oxidation of lithium ferrite occurred in a diffusion mode in a single-phase spinel structure. Therefore, in order to derive the coefficients of oxygen diffusion in ferrite, the resulting kinetic dependences  $\alpha = f(t)$  were analyzed using the solution to the second Fick's equation [21].

$$\alpha = 1 - \frac{6}{\pi^2} \sum_{n=1}^{\infty} \frac{1}{n^2} \exp\left\{-[n\pi]^2 \frac{D}{R^2} t\right\}, \quad (1)$$

where  $D$  is the diffusion coefficient,  $R$  is the particle radius, and  $t$  is the annealing time.

The calculations have shown that the temperature dependence of the effective diffusion coefficient is described by the expression  $D\ (cm^2/s) = 4.1e^{-1.88/kT}$ . For comparison, Table 2 lists the kinetic and diffusion characteristics of oxygen both for LPF2 and for nonstoichiometric lithium–titanium ferrite  $Li_{0.649}Fe_{1.598}Ti_{0.5}Zn_{0.2}Mn_{0.051}O_{4-\delta}$  ( $\Delta\delta = 0.03$ ), which were obtained using the TG method [13].

Despite the considerable differences in chemical compositions of these materials, numerical values of the parameters characterizing the diffusion-controlled oxidation of nonstoichiometric LPF and lithium–titanium spinel turned out to be quite close.

The effective activation energy of oxygen diffusion into LPF, calculated for the temperature interval  $T = (350\text{--}640)\ ^\circ\text{C}$ , was found to be  $E_D = 1.88\ \text{eV}$ . In this value, it is close to the activation energy of oxygen diffusion along grain boundaries in lithium–titanium ferrite ceramics [12, 13].

This equality of the parameters characterizing the diffusion-controlled oxidation of nonstoichiometric lithium ferrites fits well into the concepts of the governing role of the mechanism of oxygen diffusion along grain boundaries during their oxidation.

## Summary

We have shown in this work that annealing of LPF in vacuum results in oxygen nonstoichiometry of the material and its transition into a state with random distribution of cations in the crystal lattice.

In the temperature interval  $T = (350\text{--}640)\ ^\circ\text{C}$  we have derived the values of oxidation rate constants and effective coefficients of oxygen diffusion in nonstoichiometric LPF.

It has been demonstrated that the value of activation energy of oxygen diffusion in LPF samples is in a satisfactory agreement with that of the activation energy of oxygen diffusion along grain boundaries in polycrystalline lithium ferrites.

## References

- Braun PB. Superstructure in spinels. *Nature*. 1952;170:1123–4.
- Verma S, Karande J, Patidar A, Joy PA. Low-temperature synthesis of nanocrystalline powders of lithium ferrite by an auto-combustion method using citric acid and glycine. *Mater Lett*. 2005;59:2630–3.
- Levin BE, Tretyakov YuD, Levin LM. Physico-chemical mechanisms of fabrication of ferrites and their properties and application. Moscow: Metallurgiya; 1979 (in Russian).
- Baba PD, Argentina GM, Courtney WE, Dionne GF, Temme DH. Fabrication and properties of microwave lithium ferrites. *IEEE Trans Magn*. 1972;8:83–94.
- Wang X, Gao L, Li L, Zheng H, Zhang Z, Yu W, Qian Y. Low temperature synthesis of metastable lithium ferrite: magnetic and electrochemical properties. *Nanotechnology*. 2005;16:2677–84.
- Rezlescu N, Doroftei C, Rezlescu E, Popa PD. Lithium ferrite for gas sensing applications. *Sens Actuators B*. 2008;133:420–5.
- Vashman AA. Functional inorganic compounds. Moscow: Energoatomizdat; 1996 (in Russian).

8. Valenzuela R. *Magnetic ceramics*. Cambridge: Cambridge University Press; 1994.
9. West AR. *Basic solid state chemistry*. New York: Wiley; 1988.
10. Viswanathan B, Murthy VRK. *Ferrite materials science and technology*. New Delhi: Narosa Publishing House; 1990.
11. Gundlach EM, Gallagher PK. Thermogravimetric determination of the oxygen non-stoichiometry in  $\text{Ni}_{0.563}\text{Zn}_{0.188}\text{Fe}_{2.25}\text{O}_{4+\gamma}$  and  $\text{Ni}_{0.375}\text{Zn}_{0.375}\text{Fe}_{2.25}\text{O}_{4+\gamma}$ . *Thermochim Acta*. 1998;318:15–20.
12. Surzhikov AP, Lysenko EN, Ghyngazov SA, Frangulyan TS. Determination of the oxygen diffusion coefficient in polycrystalline Li-Ti ferrites. *Russ Phys J*. 2002;45:989–94.
13. Surzhikov AP, Frangulyan TS, Ghyngazov SA, Lysenko EN. Investigation of oxidation processes in non-stoichiometric lithium-titanium ferrites using TG analysis. *J Therm Anal Calorim*. 2010;102:883–7.
14. Surzhikov AP, Pritulov AM, Lysenko EN, Sokolovskiy AN, Vlasov VA, Vasendina EA. Calorimetric investigation of radiation-thermal synthesized lithium pentaferriite. *J Thermal Anal Calorim*. 2010;101:11–3.
15. Ridley DH, Lesoff H, Childress JD. Effect of lithium and oxygen losses on magnetic and crystallographic properties of spinel lithium ferrite. *J Am Ceram Soc*. 1970;53:304–11.
16. Vucinic-Vasic M, Antic B, Blanusa J, Rakic S, et al. Formation of nanosized Li-ferrites from acetylacetonato complexes and their crystal structure, microstructure and order-disorder phase transition. *Appl Phys A*. 2006;82:49–54.
17. An SY, Shim I-B, Kim CS. Synthesis and magnetic properties of  $\text{LiFe}_5\text{O}_8$  powders by a sol-gel process. *J Magn Magn Mater*. 2004;290–291:1551–7.
18. Berbenni V, Marini A, Capsoni D. Solid state reaction study of the system  $\text{Li}_2\text{CO}_3/\text{Fe}_2\text{O}_3$ . *Z Naturforsch*. 1998;53a:997–1003.
19. Cook W, Manley M. Raman characterization of  $\alpha$  and  $\beta$   $\text{LiFe}_5\text{O}_8$  prepared through a solid-state reaction pathway. *J Solid State Chem*. 2010;183:322–6.
20. Opffermann J. Kinetic analysis using multivariate non-linear regression. *J Therm Anal Calorim*. 2000;60:641–58.
21. Mianowski A, Marecka A. The isokinetic effect as related to the activation energy for the gases diffusion in coal at ambient temperatures. Part 1. Fick's diffusion parameter estimated from kinetic curves. *J Therm Anal Calorim*. 2009;95:285–92.